

Synthesis of High Aspect-Ratio Carbon Nanotube “Flying Carpets” from Nanostructured Flake Substrates

Cary L. Pint,^{†,||} Sean T. Pheasant,^{‡,||} Matteo Pasquali,^{§,||} Kent E. Coulter,[⊥]
Howard K. Schmidt,^{||} and Robert H. Hauge^{*,‡,||}

Department of Physics and Astronomy, Department of Chemistry, Department of Chemical and Biomolecular Engineering, and Richard E. Smalley Institute for Nanoscale Science and Technology, Rice University, Houston, Texas 77005, and Southwest Research Institute, San Antonio, Texas

Received February 13, 2008; Revised Manuscript Received April 16, 2008

ABSTRACT

We present a robust method for synthesis of aligned, single-walled carbon nanotube (CNT) “flying carpets” from nanostructured alumina flakes. Roll-to-roll e-beam deposition is utilized to produce the flakes, and hot filament chemical vapor deposition is utilized to grow dense, aligned carbon nanotubes from the flakes with remarkably high CNT yields. The flakes are captured inside a mesh cage and freely suspended in the gas flow during growth. Optical characterization indicates the presence of high quality, small diameter single-walled carbon nanotubes.

The growth of carbon nanotubes in architectures directly applicable into technological applications has captured much attention since their discovery. The growth of multiwalled^{2–5} and, more recently, single-walled carbon nanotubes^{6–9} in aligned arrays has brought about new opportunities for applications of these materials.^{10–12} Since the properties of aligned carbon nanotubes, including electrical and thermal conductivity and mechanical strength, are enhanced when the nanotubes are aligned,¹³ there has been much effort made to directly synthesize aligned carbon nanotube arrays and implement these materials into useful applications. In addition, aligned carbon nanotube arrays are typically grown from a catalyst that is pinned to the substrate, leaving the ultralong nanotubes grown in this method virtually free of any catalyst decoration of nanotube side-walls.

Although these materials have been studied and characterized thoroughly, there exist a number of drawbacks to their large-scale production. First and foremost, aligned carbon nanotube arrays are typically supported by a catalyst coated thin oxide layer that is evaporated onto a silicon wafer.^{8,9} In the case of vertically aligned single-walled carbon nanotube (SWNT) arrays (carpets), the mass yield of SWNTs with respect to the substrate materials is extremely low (typically

around 0.3–0.5%). As a result, the production of aligned SWNTs is inherently expensive as compared with other methods, such as chemical vapor deposition (CVD) growth on powders¹⁴ or spheroidal substrates,^{15–17} as well as processes such as high-pressure carbon monoxide (HIPCO).¹⁸ Typical yields from entangled SWNT growth on powders can be up to 30%, leaving this as being the most versatile and cost-effective from an industrial standpoint. However, SWNT growth from powders involves a catalyst with a relatively short lifetime, mostly due to the entangled nature of growth. In addition, aligned carpet growth has been achieved on spheres in CVD as well.¹⁷ Despite the high-density nature of the growth at the base of the sphere, the high-density growth can not be sustained with ultralong tubes, as the nanotube density near the top of the carpet will constantly be lower as growth proceeds. This is problematic for nanostructured spheroidal substrates and limits the yield that can be obtained.

Therefore, it is of both scientific and commercial interest to have a scalable method to produce aligned SWNT carpets which minimizes the cost and amount of substrate materials and maximizes the yield of SWNTs that can be grown from these materials. In addition, it is attractive to have a material where postgrowth processing can take place with a limited number of steps and where channels for direct applications, such as the spinning of SWNT fibers, can be realistically envisioned with a minimum number of intermediate steps. In this communication, we present the first results for such a material composed of aligned carbon nanotubes grown from

* Corresponding author. E-mail: hauge@rice.edu.

[†] Department of Physics and Astronomy, Rice University.

[‡] Department of Chemistry, Rice University.

[§] Department of Chemical and Biomolecular Engineering, Rice University.

^{||} Richard E. Smalley Institute for Nanoscale Science and Technology, Rice University.

[⊥] Southwest Research Institute.

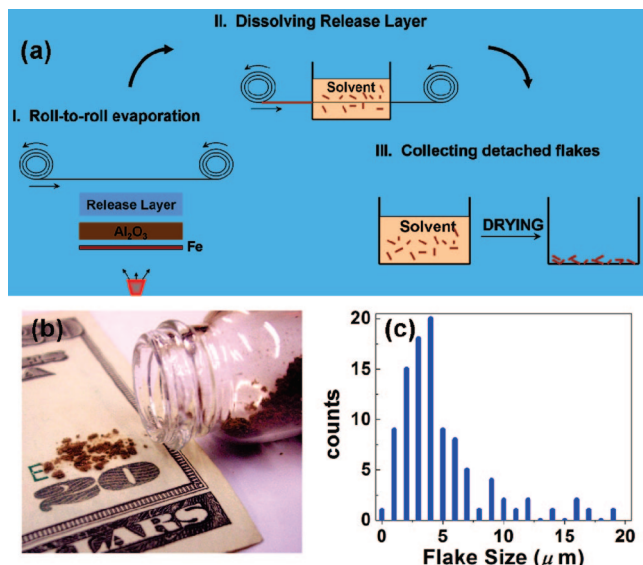


Figure 1. (a) Diagram of the process by which the flake substrates are made. The three steps of this process are the roll-to-roll deposition of the support and catalyst on a release layer (400 nm of NaCl), the dissolving of the release layer in a solvent (water) to free the catalyst coated support layer flakes, and drying the flakes. (b) Picture of flakes on a 20 dollar bill, indicating texture of dried flake material, and (c) size distribution of flakes, along the longest axis in the microstructured plane of the flake, taken by scanning electron microscopy. This distribution correlates to the diameters of individual flying carpet fibrils.

substrates that are nanostructured in one dimension (40 nm), microstructured in two other dimensions, and can be grown to aspect ratios (length/width) exceeding 100, with carbon nanotube yields greater than 400% before the occurrence of catalyst death, suggesting the possibility of even higher yields with this method. In addition, we demonstrate growth of this material that maximizes the amount of catalyst-coated substrate area contained inside of the reaction-zone volume through chemical vapor deposition where the flake substrates are free-floating in the flow of gases leading to the formation of “flying” carbon nanotube arrays or “flying carpets.”

An important aspect of the flying carpet growth is the process for making the substrates. A diagram depicting the stages of this process is shown in Figure 1a. First of all, roll-to-roll e-beam evaporation on a thin, mylar roll is utilized for a triple layer deposition. In a roll-to-roll process, the deposition rate is adjusted by both the velocity of the take-up reel and the deposition rate due to heating of the crucible with the electron beam. As a result, a 100 foot mylar roll can be used as a base material for the deposition of three layers: a release layer that can be dissolved in a solvent treatment, a catalyst support layer (Al_2O_3), and the catalyst layer (Fe). In our case, the sacrificial release layer was composed of 400 nm of NaCl, deposited directly onto an untreated, clean mylar roll. In order to produce the flakes, the release layer is dissolved away in water, detaching the thin catalyst-coated alumina layer (40 nm thick in the present case) into flakes, which can then be dried, filtered, and collected. The filter utilized removed all flakes in excess of 20 μm . The flakes are then ground in a mortar and pestle and ready for CVD growth. Figure 1b shows a picture of

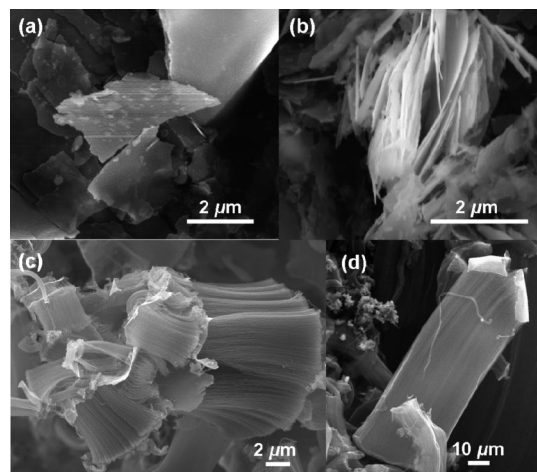


Figure 2. (a) Top-view and (b) side-view (of a cluster) scanning electron microscope (SEM) images of flakes produced in the roll-to-roll process. Notice the transparent nature of the flake in (a) to the underlying flakes. (c,d) SEM images of typical low-aspect ratio fibrils grown at the lowest CVD growth gas pressure. Notice the broken flake in (d) representing stresses in the fibrils as their diameters become large.

the flakes on a 20 dollar bill, and Figure 1c shows a distribution of flake sizes, taken from 101 flakes with a scanning electron microscope (SEM) where the reported size is along the longest direction in the microstructured plane of the flake. From SEM images, the majority of flakes are between 1–8 μm in width, with a small quantity of larger flakes present as well. It should be noted that this width directly controls the diameter of the flying carpets grown in CVD, giving indication for the sizes of flying carpets typically grown in this method.

Flying carpets were synthesized in a hot filament chemical vapor deposition apparatus. This type of apparatus has been described in detail elsewhere¹⁹ but relies upon atomic hydrogen for the rapid reduction of the Fe_2O_3 catalyst into metallic Fe for efficient growth of small diameter, single-walled carbon nanotubes. Prior to growth, the flake material is loaded into a mesh cage, where the growth gases can penetrate the cage, but with mesh pores small enough that reasonable growth rates of nanotubes in the flying carpets will keep them confined inside the cage once lift-off occurs in the flow of growth gas. An image of a typical mesh cage utilized for growth is shown in Supporting Information.

Figure 2a,b shows side- and top-view SEM images of the flakes prior to growth. The thin nature of the flake can be noticed in Figure 2a, as it is somewhat transparent to the larger flake it is sitting on. SEM images shown in Figure 2c,d are images of some low-aspect-ratio flying carpets that are obtained by growth at 1.4 Torr reaction zone pressure, after 30 and 150 min of growth, respectively. In general, we observe that growth of flying carpets in the hot-filament CVD apparatus mimics growth of vertically aligned SWNTs from flat Si-supported wafers, in that changes in the growth conditions, time, temperature, and gas pressure, are directly related to features of the nanotubes that are grown. As a result, the duration of growth time, pressure of gas inside of the reaction zone, or both are parameters that can be changed

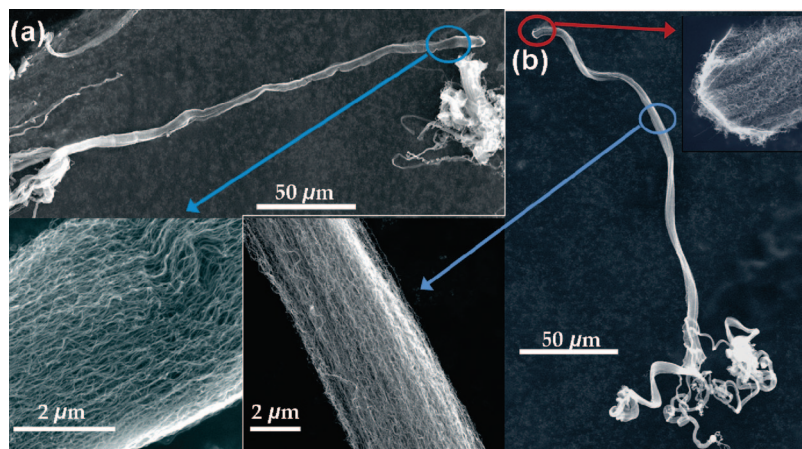


Figure 3. (a,b) SEM images of high aspect-ratio flying carpet fibrils and accompanying high-magnification images of carbon nanotube bundles making up the fibrils. The end of the fibril containing the catalyst coated flake is also inset in (b). Note the twists and curls in the high aspect-ratio fibrils.

to enhance the length of the nanotubes grown in the flying carpets. Figure 3 shows SEM images of some typical high-aspect-ratio flying carpets grown in the CVD reactor. In both cases, the diameters of the flying carpets are between 5–7 μm , which corresponds well to the most abundant flake sizes shown in Figure 1. However, in SEM images presented in both a and b of Figure 3, the lengths of the flying carpets are well over 200 μm , yielding aspect ratios (length/width) greater than 40. One intrinsic feature of the growth of nanotube arrays from these nanostructured flakes is that the flying carpets are not constrained in a geometry that is dictated by the substrate, but rather free to grow in such a way as to minimize the stresses associated with the growth of a SWNT carpet from a coated Si wafer. This is apparent in Figure 3, as the flying carpet “filaments” tend to be twisted or curled at some points. It was generally observed that filaments with aspect ratios comparable to or larger than those shown in Figure 3 tended to coil on themselves. This resulted in difficulty in measuring the total length of such a fibril. However, under pressures ranging between 1.4 and 15 Torr, with growth times of 150 min, typical distributions of flying carpets were between 50 and 400 μm , with cross-sectional diameters ranging between 1 and 20 μm .

Also important for the flying carpets presented here are the features of the nanotubes themselves, specifically, the quality of the nanotubes as measured by Raman spectroscopy, as well as some indication of the nanotube diameters present in the flying carpets. The focus of characterization of the nanotubes will be those grown under optimal conditions for SWNT growth in reaction pressures of 1.4 Torr (images presented in Figure 2). Further characterization of flying carpet growth at higher pressures is available in Supporting Information. Figure 4a shows Raman spectra, taken with a 785 nm laser in a Kaiser fiber-optic liquid Raman device. Here, the flying carpets were dispersed in 1 wt % sodium deoxycholate by tip sonication and centrifuged at 12 000 RPM for 75 min. This treatment was observed to be enough to remove residual flakes, particulates, or both from the solution containing the dispersed nanotubes. The resulting G/D ratio is high for this dispersion, yielding a value

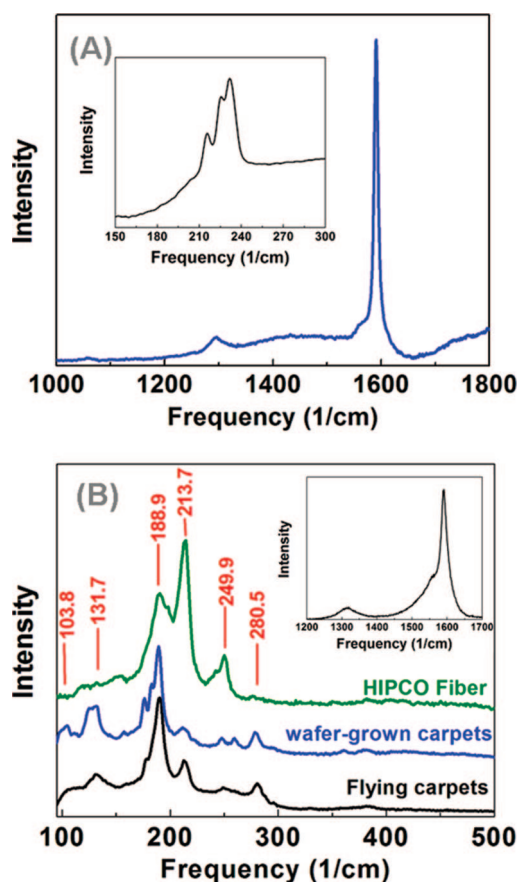


Figure 4. (a) Raman spectroscopy of the D and G peaks of surfactant suspended flying carpets with 785 nm optical excitations from an optical probe. Radial breathing modes (RBM) are inset. (b) Raman spectroscopy comparing RBM spectra of as-grown flying carpet fibrils, as-grown wafer-supported carpets, and a neat, aligned SWNT fiber spun from nanotubes grown in HIPCO, using a 633 nm laser. Inset in (b) is the D and G bands of the solid flying carpet material, for comparison to (a).

of approximately 35 after subtracting the baseline noise from both D and G peaks. It should be noted that there is a broad peak between the G and D peak in the spectra shown in Figure 4a that is due to fluorescence emission from a small diameter semiconducting SWNT overlapping with the Raman

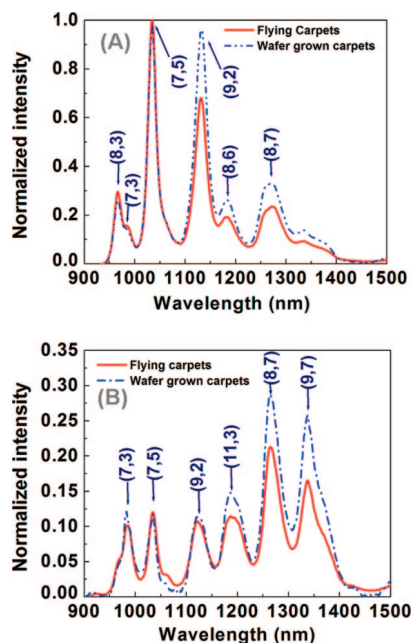


Figure 5. Comparison of fluorescence emission spectra of surfactant suspended flying carpet SWNTs and flat, Si wafer grown SWNTs utilizing the same growth conditions, with (a) 660 nm excitations and (b) 780 nm excitations. The (n,m) assignments are made to the most apparent emission peaks corresponding to individual SWNTs.

spectra. However, this indicates that the nanotubes grown in the flying carpets are of comparable quality to entangled nanotubes grown in processes such as HIPCO or CoMoCat.²⁰ Also inset in Figure 4a are radial breathing modes (RBM) from 785 nm liquid Raman, indicating the presence of single-walled carbon nanotubes in the flying carpets. This is better presented by Figure 4b, which shows RBMs of the same flying carpet material, except in a solid form with no surfactant suspension, compared with as-grown wafer carpets and a fiber spun from aligned HIPCO SWNTs. With a 633 nm laser, there are several RBMs evident, six of which are assigned to frequencies corresponding to nanotubes with diameters ranging between 0.6 and 1.8 nm. In addition, the wafer-grown carpets seem to have a similar RBM spectrum to the flying carpets, except the RBM frequencies corresponding to the largest nanotubes (near 100 cm^{-1}) seem to be almost absent for the flying carpets. In addition, the D and G peaks for the solid flying carpet material inset in Figure 4b indicate a G/D ratio of approximately 10. By comparing this with the G/D ratio established through liquid Raman measurements of dispersed SWNTs, this suggests the presence of a reasonable amount of amorphous carbon in the as-grown sample. However, a G/D ratio of 10 in the as-grown material is still indicative of the presence of high quality SWNTs.

The observation of high-quality, small-diameter, single-walled carbon nanotubes in Raman spectroscopy is further emphasized by fluorescence spectra shown in Figure 5. Since only semiconducting, single-walled carbon nanotubes are known to fluoresce,^{21,22} we utilized optical excitations at 660 and 785 nm to monitor the presence of surfactant-suspended SWNTs from flying carpets. The (n,m) assignments for

individual fluorescence peaks shown in Figure 5 indicate that the flying carpets are rich in semiconducting SWNTs. A comparison of flying carpet SWNTs to SWNTs grown in carpets on Si-supported wafers under the same conditions indicates only a slightly different relative population of SWNTs, shifted more toward the smaller diameter nanotubes (which are assigned to peaks at lower emission wavelengths), consistent with the general observations made through the RBMs in Figure 4b. One possible reason for the smaller diameter SWNTs present in flying carpets is that the deposition rate in the roll-to-roll e-beam deposition apparatus is greater than that used in e-beam deposition of Fe on a solid wafer (typically 0.5 $\text{\AA}/\text{s}$). This could lead to more nucleation sites for Fe island growth on Al_2O_3 , leading to smaller overall catalyst size in the roll-to-roll process.

We also observe there is good consistency between the flying carpet material and the wafer-supported carpets in the sense that changes of growth conditions, in particular, increasing gas pressure inside the reaction zone, leads to lower values for G/D ratios and evidence of more few-wall nanotubes and larger diameter SWNTs being grown (see Supporting Information). This consistency means that the growth observed in flying carpets can be understood in the same phenomenological framework as that which has been developed for wafer supported carpets.^{23,24} This means that, as we demonstrate, optimum growth conditions (highest growth temperatures, lowest carbon flux) can be achieved to yield growth of purely single-walled carbon nanotubes. However, by only changing a few parameters (lowering the temperature and/or increasing carbon flux), one can just as easily grow larger diameter SWNTs and few-walled nanotubes.

Even though it is more often than not desired to have high quality SWNTs in the carpet, there are some applications where a high productivity of SWNTs along with two- and three-walled carbon nanotubes is attractive. One example of such an application is in field emission displays, where the exceptional high aspect ratio of such nanotubes is sought. High resolution transmission electron microscope images of carbon nanotubes grown from flying carpet substrates at 25 Torr indicate that there is a mixture of small-diameter SWNTs (diameter less than 1.5 nm) and large diameter SWNTs (diameters between 1.5–6 nm), as well as few-walled multiwalled carbon nanotubes, present under such conditions. Under such conditions, G/D ratios also decrease to below 2, indicative of a higher D band which we typically observe to be characteristic of multiwalled carbon nanotube presence. However, growth at 25 Torr for 180 min yields over four times the mass of nanotubes than the starting material, as measured by a precision balance (i.e., over a 400% yield of nanotubes relative to the starting substrate materials). Starting with only 3.4 mg of flake material, we can produce 18.6 mg of combined flakes and nanotubes. This is reproducible with growth at 12 Torr as well, where after 300 min of growth, a similar yield is obtained. By comparing the yield of nanotubes between growth at 1.4 Torr (high quality SWNTs) and 25 Torr reaction pressures for a growth duration of 60 min, the yields were 41% and 129%, respectively. It is important to also note that the duration of

growth at 1.4 Torr reaction pressure for wafer supported carpets has been found to exceed 6 h, suggesting that the potential SWNT yields that can be achieved by this method are much higher than those reported here.

In addition, we have also grown flying carpets with catalyst layer thicknesses of up to 5 nm. SEM images of flying carpets grown from thick catalyst layers (see Supporting Information) supports the growth of large diameter, multi-walled carbon nanotubes from this catalyst thickness and under conditions of the lowest pressure. As a result, we have shown that both reaction zone pressure and catalyst thickness can be varied to grow SWNTs and few-walled carbon nanotubes, as well as large MWNTs, in a similar way to carpet growth but from nanostructured substrates made by a roll-to-roll deposition technique.

Finally, it is interesting to consider the scalability of such a scheme. Our choice of Al_2O_3 as a flake material is due to vast literature indicating that an Al_2O_3 support layer is typically the best for carpet growth. However, other materials, such as MgO ²⁵ or TiN ²⁶ have been shown to be possible supports for carpet growth as well. MgO is interesting because it can be removed in a light HCl etch, similar to that of the Fe_2O_3 catalyst. This would mean that processing of nanotubes from flying carpet materials grown on MgO supports could undergo one-step liquid processing for removal of both catalyst and substrate. In addition, growth on conductive supporting layers, such as TiN , could be directly implemented into electronic applications since growth takes place on a conductive substrate. In any case, we show here a robust method for producing nanostructured flakes that can support carpet growth without the stranglehold of entangled growth from nanostructured spheroidal substrates,^{15–17} as well as the low nanotube yield of carpets from flat, coated Si wafers. We show that hot filament chemical vapor deposition is an efficient route for producing flying carpets and that high quality, small diameter, SWNT populated flying carpets can be synthesized, with high aspect ratios, under optimum conditions for SWNT growth.

Acknowledgment. The authors would like to thank D. Natelson's group for use of equipment. Also, thanks to N. Nicholas, J. Duque, N. Parra-Vasquez, and N. Alvarez for insightful discussions and thoughts on this work, and thanks to R. Booker for the HIPCO fiber. This work is funded under Air Force OSB Grant FA9550-06-1-0207.

Supporting Information Available: Additional experimental details, additional characterization (TEM, Raman

spectroscopy, and fluorescence data), and additional SEM images of multiwalled carbon nanotube fibrils and SWNT fibrils are available. Also available is a schematic of an optimal reactor for highly productive flying carpet growth. This material is available free of charge via the Internet at <http://pubs.acs.org>.

References

- (1) Iijima, S. *Nature* **1991**, 354, 56–58.
- (2) Li, W. Z.; Xie, S. S.; Qian, L. X.; Chang, B. H.; Zou, B. S.; Zhou, W. Y.; Zhao, R. A.; Wang, G. *Science* **1996**, 274, 1701.
- (3) Pan, Z. W.; Xie, S. S.; Chang, B. H.; Wang, C. Y.; Lu, L.; Wu, W.; Zhou, W. Y.; Li, W. Z.; Qian, L. X. *Nature* **1998**, 394, 631.
- (4) Zhang, X.; Cao, A.; Wei, B.; Li, Y.; Wei, J.; Xu, C.; Wu, D. *Chem. Phys. Lett.* **2002**, 362, 285.
- (5) Christen, H. M.; Puzos, A. A.; Cui, H.; Belay, K.; Fleming, P. H.; Geohegan, D. B.; Lowndes, D. H. *Nano Lett.* **2004**, 4, 1939.
- (6) Murakami, Y.; Chiashi, S.; Mayauchi, Y.; Hu, M.; Ogura, M.; Okubo, T.; Maruyama, S. *Chem. Phys. Lett.* **2004**, 385, 298.
- (7) Hata, K.; Futaba, D. N.; Mizuno, K.; Namai, T.; Yumura, M.; Iijima, S. *Science* **2004**, 306, 1362–1364.
- (8) Eres, G.; Kinkhabwala, A. A.; Cui, H.; Geohegan, D. B.; Puzos, A. A.; Lowndes, D. H. *J. Phys. Chem. B* **2005**, 109, 16684.
- (9) Xu, Y. Q.; Flor, E.; Kim, M.; Hamadani, B.; Schmidt, H.; Smalley, R. E.; Hauge, R. *J. Am. Chem. Soc.* **2006**, 128, 6560.
- (10) Ge, L.; Sethi, S.; Ci, L.; Ajayan, P. M.; Dhinojwala, A. *Proc. Natl. Acad. Sci.* **2007**, 104, 10792.
- (11) Qu, L.; Dai, L. *Adv. Mater.* **2007**, 19, 3844.
- (12) Majumder, M.; Chopra, N.; Andrews, R.; Hinds, B. J. *Nature* **2005**, 438, 44.
- (13) Choi, E. S.; Brooks, J. S.; Eaton, D. L.; Al-Haik, M. S.; Hussaini, M. Y.; Garmestani, H.; Li, D.; Dahmen, K. *J. Appl. Phys.* **2003**, 94, 6034.
- (14) Liu, B. C.; Liu, S. C.; Jung, S. I.; Kang, H. K.; Yang, C.-W.; Park, J. W.; Park, C. Y.; Lee, C. J. *Chem. Phys. Lett.* **2004**, 383, 104.
- (15) Huang, S. *Carbon* **2003**, 41, 2347.
- (16) Agrawal, S.; Kumar, A.; Frederick, M. J.; Ramanath, G. *Small* **2005**, 1, 823.
- (17) Xiang, R.; Luo, G. H.; Qian, W. Z.; Wang, Y.; Wei, F.; Li, Q. *Chem. Vap. Deposition Comm.* **2007**, 13, 533.
- (18) Nikolaev, P.; Bronikowski, M. J.; Bradley, R. K.; Rohmund, F.; Colbert, D.; Smith, K. A.; Smalley, R. E. *Chem. Phys. Lett.* **1999**, 313, 91.
- (19) Xu, Y.-Q.; Flor, E.; Kim, M.; Hamadani, B.; Schmidt, H.; Smalley, R. E.; Hauge, R. H. *J. Am. Chem. Soc.* **2006**, 128, 6560.
- (20) Herrera, J. E.; Resasco, D. E. *Chem. Phys. Lett.* **2003**, 376, 302.
- (21) Bachilo, S. M.; Strano, M. S.; Kittrell, C.; Hauge, R. H.; Smalley, R. E.; Weisman, R. B. *Science* **2002**, 298, 2361.
- (22) Dmitri, A., (unpublished).
- (23) Puzos, A. A.; Geohegan, D. B.; Jesse, S.; Ivanov, I. N.; Eres, G. *Appl. Phys. A: Mater. Sci. Process.* **2005**, 81, 223.
- (24) Wood, R. F.; Pannala, S.; Wells, J. C.; Puzos, A. A.; Geohegan, D. B. *Phys. Rev. B* **2007**, 75, 235446.
- (25) Milne, W. I.; Teo, K. B. K.; Minoux, E.; Groening, O.; Gangloff, L.; Hudanski, L.; Schnell, J.-P.; Dieumegard, D.; Peauger, F.; Bu, I. Y. Y.; Bell, M. S.; Legagneux, P.; Hasko, G.; Amarutunga, G. A. J. *J. Vac. Sci. Technol. B* **2006**, 24, 345.
- (26) Xiong, G.-Y.; Wang, D. Z.; Ren, Z. F. *Carbon* **2006**, 44, 969.

NL0804295